Vector spectral functions at finite temperature

Harvey Meyer
Johannes Gutenberg University Mainz

German-Japanese Workshop 2024, Mainz, 25 September 2024

This talk is mainly based on the following publications:

1. 2001.03368 (PRD): *Rate of photon production in the quark-gluon plasma from lattice QCD*,
   Marco Cè, Tim Harris, HM, Aman Steinberg, Arianna Toniato.

2. 2205.02821 (PRD): *Photon emissivity of the quark-gluon plasma: A lattice QCD analysis of the transverse channel*,
   Marco Cè, Tim Harris, Ardit Krasniqi, HM, Csaba Török.

3. 2309.09884 (PRD): *Probing the photon emissivity of the quark-gluon plasma without an inverse problem in lattice QCD*,
   Marco Cè, Tim Harris, Ardit Krasniqi, HM, Csaba Török.

4. 2407.01657: *Hot QCD matter around the chiral crossover: A lattice study with O(a)-improved Wilson fermions*,
   Ardit Krasniqi, Marco Cè, Renwick Hudspith, HM.

Polarisation tensor at finite temperature and photon emissivity

$$\rho^{\mu\nu}(\omega,\boldsymbol{k}) = \int d^4x\, e^{i(\omega x^0 - \boldsymbol{k}\cdot\boldsymbol{x})}\, \frac{1}{Z}\sum_n e^{-E_n/T}\langle n|[j^\mu(x), j^\nu(0)]|n\rangle$$

- at finite temperature, there are two independent, O(3) invariant components: $(k \equiv |\boldsymbol{k}|, \quad \hat{k}^i = k^i/k)$

$$\rho_L(\omega,k) \equiv (\hat{k}^i\hat{k}^j\rho^{ij} - \rho^{00}), \qquad \rho_T(\omega,k) \equiv \frac{1}{2}(\delta^{ij} - \hat{k}^i\hat{k}^j)\rho^{ij}.$$

- current conservation: $\omega^2\rho^{00}(\omega,k) = k^i k^j \rho^{ij}(\omega,k)$ implies that ρ_L vanishes at lightlike kinematics, $\mathcal{K}^2 = 0$.

- Photon emissivity can be written [McLerran, Toimela 1985]

$$d\Gamma_\gamma(\boldsymbol{k}) = \alpha\, \frac{d^3k}{2\pi^2\, k}\, \frac{\sigma(k)}{e^{\beta k} - 1},$$

$$\sigma(k) \equiv (\rho_T + \tfrac{\lambda}{2}\rho_L)(\omega = k, k) \qquad (\forall\lambda).$$

Predictions for $\sigma(k)$ in non-Abelian plasmas:

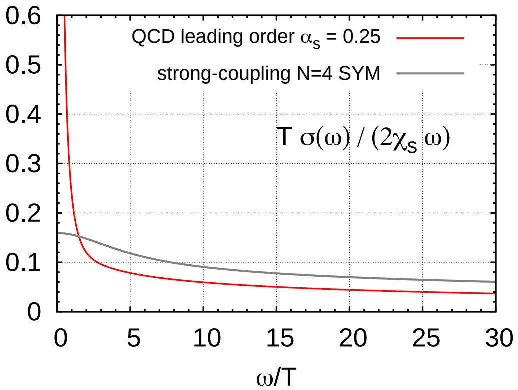

intercept $= T \cdot D$,

$D =$ diffusion coefficient.

- $\sigma(\omega)$ vanishes in the vacuum;
- at $\omega \neq 0$ it vanishes for thermal, non-interacting quarks;
- ideal probe of the medium!

Arnold, Moore Yaffe JHEP 11 (2001) 057; JHEP 12 (2001) 009. NLO: Ghiglieri et al 1302.5970.
AdS/CFT: Caron-Huot et al. JHEP 12 (2006) 015.

Lattice QCD and vector correlators

Imaginary-time path-integral representation of QFT (Matsubara formalism).

Imaginary-time **vector correlators** ($\{\gamma^\mu, \gamma^\nu\} = 2g^{\mu\nu} = 2\mathrm{diag}(1, -1, -1, -1)$),

$$G^{\mu\nu}(x_0, \boldsymbol{k}) = \int d^3x \; e^{-i\boldsymbol{k}\cdot\boldsymbol{x}} \, \mathrm{Tr}\Big\{ \frac{e^{-\beta H}}{Z(\beta)} j^\mu(x)\, j^\nu(0) \Big\}, \qquad j^\mu = \sum_f Q_f \, \bar\psi_f \gamma^\mu \psi_f$$

Spectral representation at fixed spatial momentum $\boldsymbol{k}$: (u is a real four-vector)

$$u_\mu G^{\mu\nu} u_\nu(x_0, \boldsymbol{k}) = \int_0^\infty \frac{d\omega}{2\pi} \; \underbrace{\frac{(u_\mu \rho^{\mu\nu} u_\nu)(\omega, \boldsymbol{k})}{\sinh(\beta\omega/2)}}_{\geq 0} \; \cosh[\omega(\beta/2 - x_0)].$$

$\rightsquigarrow$ **inverse problem.**

Studied on the lattice at $\boldsymbol{k} \neq 0$ since Aarts et al hep-lat/0610061.

Choosing λ: weak and strong coupling spectral functions

Spatial momentum $k = \pi T$: (see Caron-Huot et al '06 and Laine 1310.0164)

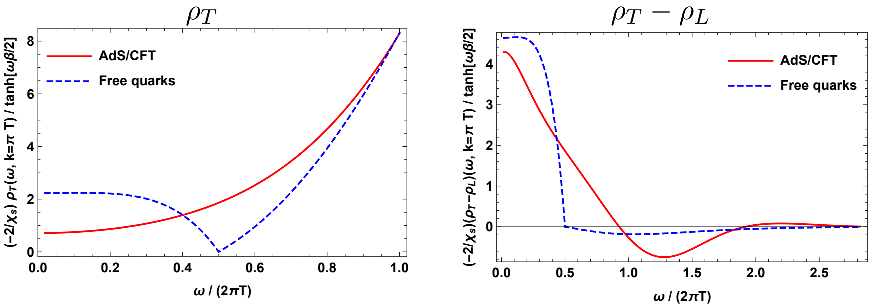

- ρ_T is positive-definite and free of the diffusion pole
- $(\rho_T - \rho_L)$ vanishes in the vacuum, is strongly suppressed at large ω and obeys a superconvergent sum-rule.
- At $\omega = k$, the two channels should be equal: non-trivial consistency check for lattice-based calculations!

Parameters of the lattice calculations

- $N_f = 2$ flavours of dynamical O(a) improved Wilson fermions with Wilson gauge action; ensembles generated with the openQCDv1.6 code.
- $T \simeq 254\,$MeV, $L = 4/T \simeq 3.1\,$fm; $m_\pi(T = 0) \simeq 270\,$MeV.
- Isovector current correlator is computed.

label	$1/(aT)$
F7	12
O7	16
W7	20
X7	24

See 2001.03368 $(\rho_T - \rho_L)$, and 2205.02821 (ρ_T).

Final result of analysis of the $(\rho_T - \rho_L)$ channel

$$D_{\rm eff}(k) \equiv \frac{\rho(\omega = k, k, \lambda)}{4\chi_s k}, \qquad \chi_s = \beta \int d^3x \langle V_0(x) V_0(0)\rangle.$$

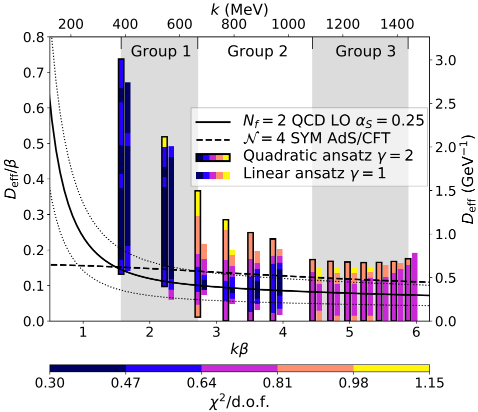

Cè et al. 2205.02821 (PRD).

Final result for the photon emissivity from the transverse channel

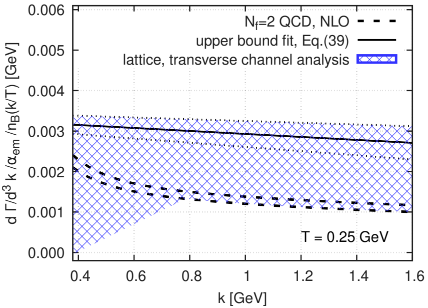

- The band represents the spread resulting from 68% of successful fits.
- Most fits give a larger photon emissivity than the weak-coupling prediction, but overall the lattice result is still compatible with it.
- The AdS/CFT prediction is also consistent with the lattice data for $k \gtrsim \pi T/2$.

2205.02821 Török et al.

A dispersion relation for a Euclidean correlator at zero virtuality

- let

$$H_E(\omega_n) \equiv -\int_0^\beta dx_0 \int d^3x\, e^{\omega_n(ix_0+x_3)}\ \langle j_1(x) j_1(0)\rangle$$

be the momentum-space Euclidean correlator with *imaginary* spatial momentum $k = i\omega_n$;

- once-subtracted dispersion relation: $(\sigma(\omega) \sim \omega^{1/2}$ at weak coupling)

$$H_E(\omega_n) = -\frac{\omega_n^2}{\pi}\int_0^\infty \frac{d\omega}{\omega}\, \frac{\sigma(\omega)}{\omega^2+\omega_n^2}\,.$$

- these energy-moments of $\sigma(\omega)$ are directly accessible without involving an inverse problem.

HM, 1807.00781 (EPJC).

How different energy-moments probe $\sigma(\omega)$

$$H_E(\omega_r) - H_E(\omega_n) = \int_0^\infty \frac{d\omega}{\pi} \left[\frac{\omega_n^2}{\omega^2+\omega_n^2} - \frac{\omega_r^2}{\omega^2+\omega_r^2} \right] \frac{\sigma(\omega)}{\omega}.$$

$$\swarrow \qquad\qquad\qquad \downarrow$$

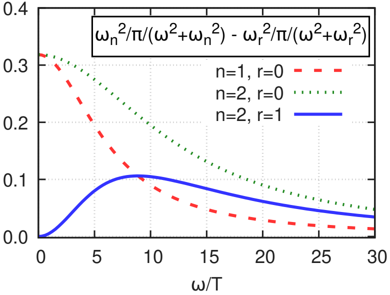

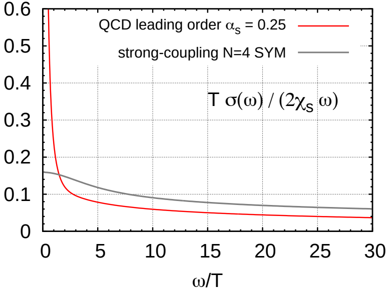

- $H_E(\omega_1)$ receives a sizeable contribution from the soft photons;
- $H_E(\omega_2) - H_E(\omega_1)$ probes the emission of hard photons.

Formulation on the lattice

Our standard representation: [Cè, ... HM, 2112.00450]

$$-H_E(\omega_n) = \int_0^\beta dx_0 \int d^3x \, (e^{i\omega_n x_0} - e^{i\omega_n x_2}) \, e^{\omega_n x_3} \, \langle j_1(x) j_1(0) \rangle.$$

The $e^{i\omega_n x_2}$ term subtracts a static contribution which vanishes in the continuum (for the same reason the polarisation tensor component $\Pi_{11}(q)$ vanishes at lightlike virtuality for $q_1 = 0$).

- This representation has the advantage that $H_E(\omega_n)$ vanishes exactly in the vacuum even at finite lattice spacing;
- as a consequence, cutoff effects at finite temperature are strongly reduced.

Final integrand in variable x_3 to compute $-H_E(\omega_1)$:

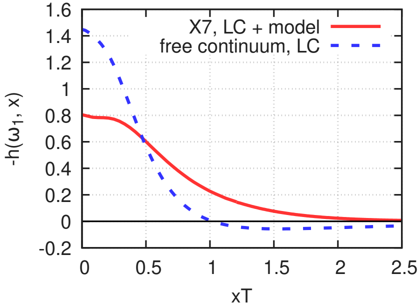

Computing $H_E(\omega_1)$ $N_f = 2$, $T = 254\mathrm{MeV}$, $N_t = 16, 20, 24.$

Effective masses $\frac{1}{a}\log\frac{h(\omega_1,x_3)}{h(\omega_1,x_3+a)}$

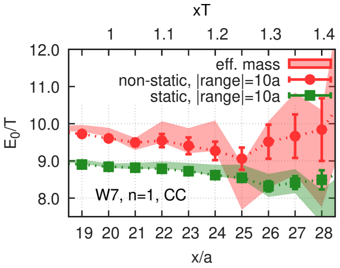

Treatment of integrand at long distances

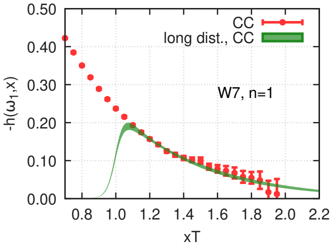

Continuum extrapolation using three discretisations of the vector correlator

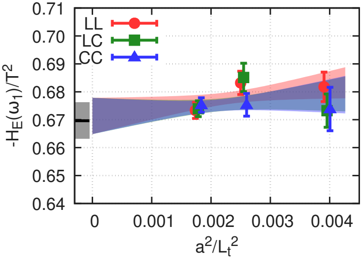

Result for $H_E(\omega_1)$: comparison to strong/weak-coupling predictions

- Our result: $-H_E(\omega_1)/T^2 = 0.670(6)_{\rm stat}(1)_{\rm syst}$

  vs.

  $$-H_E^{\rm AMY}(\omega_1)/T^2 = 0.75\dots 0.89$$

(for $\alpha_s \doteq 0.25...0.31$, integrating over $0.2 \le \omega/T \le 50$)

- Comparing to strongly coupled, $N_c = \infty$, $\mathcal{N} = 4$ SYM: normalize by static susceptibility

our result: $-H_E(\omega_1)/\chi_s = 0.76(2)$

vs.

$$-H_E^{\rm SYM}(\omega_1)/\chi_s = 0.6715.$$

- $-H_E(\omega_1)$ is clearly smaller than the value predicted from the AMY spectral function $\sigma(\omega)$ using $\alpha_s = 0.25\dots 0.31$.
- for $H_E(\omega_2)$: better control of the large x_3 regime needed.

Cè et al, 2309.09884 (PRD).

Study of spectral functions across the thermal crossover

- $N_f = 2 + 1$ flavours of dynamical O(a) improved Wilson fermions with treelevel improved Lüscher-Weisz gauge action; ensembles generated with the openQCDv2.0 code;
- $m_\pi(T = 0) = 130\,\mathrm{MeV}$, $m_K(T = 0) = 489\,\mathrm{MeV}$;
- $T \simeq 128,\ 154,\ 192\,\mathrm{MeV}$, $L = 96a = 6.1\,\mathrm{fm}$; $a = 0.064\,\mathrm{fm}$;
- Isovector current correlators are computed.

Backus-Gilbert method to construct a smeared spectral function from the Euclidean correlator:

$$\frac{\hat{\rho}(\bar{\omega})}{\bar{\omega}} = \sum_{i=1}^{N_p} q_i(\bar{\omega}) G(\tau_i) = \int_0^\infty \mathrm{d}\omega\, \hat{\delta}(\bar{\omega}, \omega) \frac{\rho(\omega)}{\omega}\,,$$

with

$$\int_0^\infty d\omega\, \hat{\delta}(\bar{\omega}, \omega) = 1.$$

Phenomenological vacuum spectral functions

Vector

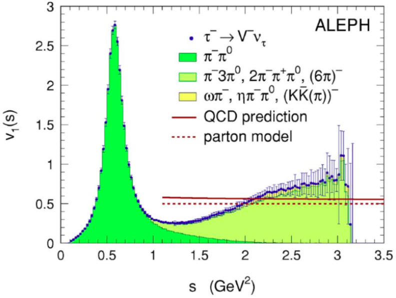

Axial-vector

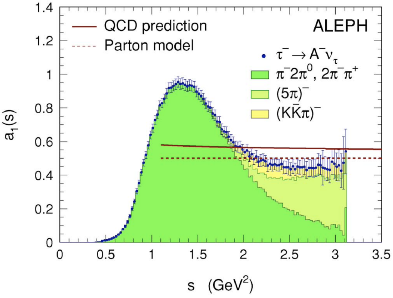

Figs. from Davier, Höcker, Zhang DOI:10.1103/RevModPhys.78.1043

Connection with vector spectral functions $\rho(\omega, T=0)$ on the next slide:

$$-\int d^3x \left\langle \bar{\psi}(x)\gamma_j \tfrac{\tau^b}{2}\psi(x)\ \bar{\psi}(0)\gamma_i \tfrac{\tau^a}{2}\psi(0) \right\rangle = \delta^{ab}\delta_{ij} \int_0^\infty d\omega\, \rho(\omega,0)\, e^{-\omega x_0},$$

$$\rho(\omega,0) = \frac{1}{4\pi^2}\omega^2 v_1(\omega^2).$$

Thermal modification of the vector spectral function

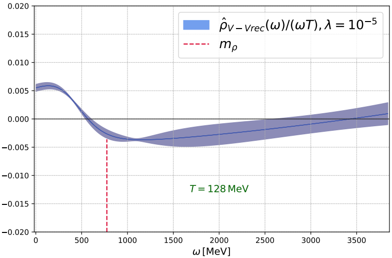

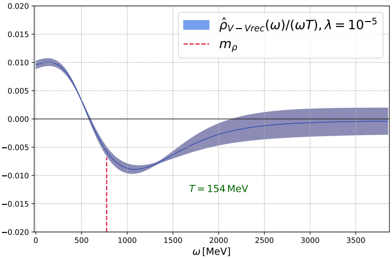

Use spatial components $\bar{\psi}\gamma_i\psi$ at $\boldsymbol{k} = 0$;

$$\Delta\rho(\omega, T) \equiv \rho(\omega, T) - \rho(\omega, 0);$$

$$\int_0^\infty \frac{\mathrm{d}\omega}{\omega}\,\Delta\rho_V(\omega, T) = 0$$

[1107.4388 Bernecker, HM;
2407.01657 Krasniqi et al.]

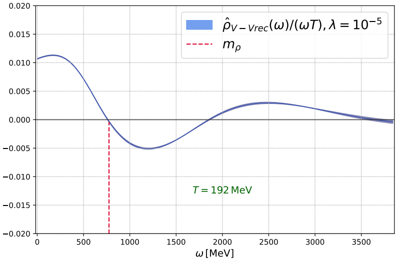

Idem for the axial-vector spectral function

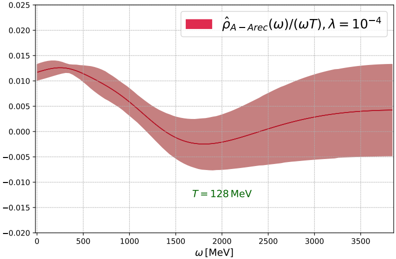

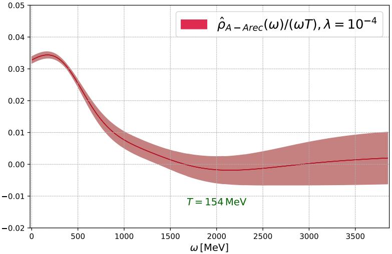

Behaviour consistent with the sum rule

$$2\int_0^\infty \frac{\mathrm{d}\omega}{\omega}\,\Delta\rho_A(\omega,T)$$
$$= f_\pi^2(T=0) - f_\pi^2(T) + \mathcal{O}(m_q^2).$$

Screening pion decay constant $f_\pi(T)$ is small for $T \gtrsim 140\,\mathrm{MeV}$.

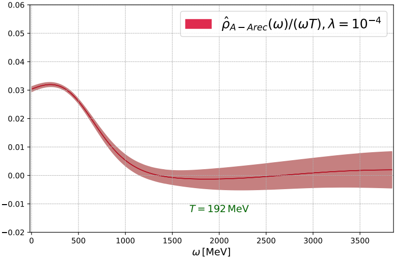

Conclusion

- Electromagnetic current two-point correlators:
  lattice calculations with fully dynamical quarks and the continuum limit.
- Dispersion relation at fixed photon virtuality $q^2 = 0$:
  the photon-energy moment $|H_E(\omega_1)|$ is smaller than the value derived from the weak-coupling spectral function $\sigma_{\rm AMY}(\omega)$.
- Thermal modification of vector and axial-vector spectral functions at physical quark masses: Backus-Gilbert-smeared spectral functions qualitatively consistent with sum rules.

The axial-charge correlator

$$A_0^a = \bar{\psi}\gamma_\mu\gamma_5 \tfrac{\tau^a}{2}\psi,\ \ \psi = \begin{pmatrix} u \\ d \end{pmatrix};$$

$$\int d^3x\, e^{-i\boldsymbol{k}\cdot\boldsymbol{x}}\, \langle A_0^a(x) A_0^b(0)\rangle =$$

$$\delta^{ab} \int_0^\infty d\omega\, \rho_{A_0}(\omega, \boldsymbol{k})\, \frac{\cosh[\omega(\beta/2 - x_0)]}{\sinh(\beta\omega/2)}$$

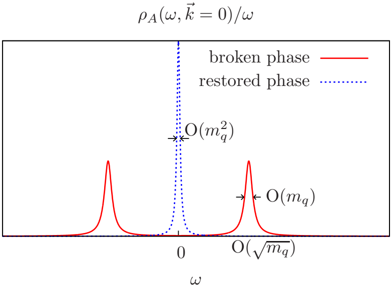

Near the chiral limit $m_q = 0$:

- below the thermal transition: propagating mode, the 'pion quasiparticle'; [Son, Stephanov hep-ph/0204226]
- above the transition: chiral symmetry is restored $\Rightarrow$ at $m_q = 0$, ρ_{A_0} is degenerate with the isovector vector spectral function, $\rho_{V_0}(\omega, \mathbf{0}) = \chi_s \omega \delta(\omega)$; the mode is purely diffusive. [Krasniqi et al. 2407.01657]

The low-lying non-static screening spectrum

$$h_{\rm ns}(\omega_r, x_3) = \sum_n |A_n^{(r)}|^2 \, e^{-E_n^{(r)}|x_3|} > 0.$$

In Matsubara sector $\omega_r = 2\pi T r$, $r \in \mathbb{Z}$: $E_n^{(r)} \geq \omega_r$ (causality).

In $r = 2$ sector, possible kinematic configurations:

- quark with momentum $p_0 = \pi T$, antiquark with momentum $p_0 = 3\pi T$, or the other way around.
- Low-lying states: at high T, physics of (p-wave) quarkonia in 2+1d, with a $q\bar{q}$ potential mediated by static gluons.
- higher up, the spectrum becomes continuous; first threshold due to scattering states of two $r = 1$ screening states.

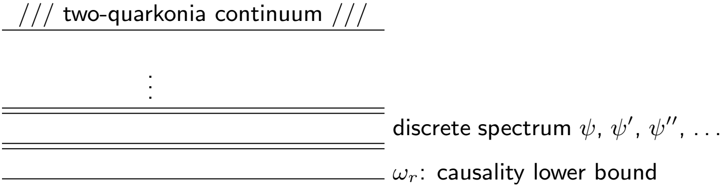

Continuum extrapolation of the $\rho_T - \rho_L$ Euclidean correlator

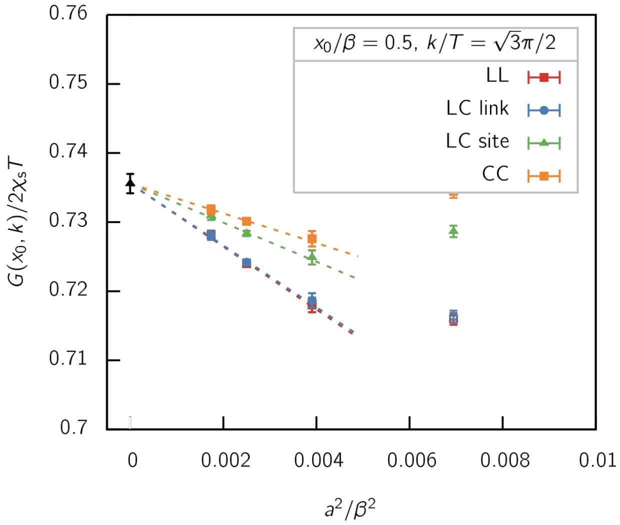

Analysis of the $(\rho_T - \rho_L)$ channel

'Hydrodynamics' prediction at small ω, k: with D the diffusion coefficient,

$$\rho(\omega, k, -2)/\omega \approx \frac{4\chi_s\, Dk^2}{\omega^2 + (Dk^2)^2} \qquad \omega, k \ll D^{-1}.$$

From the operator-product expansion:

$$\rho(\omega, k, \lambda = -2) \overset{\omega\to\infty}{\sim} k^2/\omega^4 \;\; : \qquad \int_0^\infty d\omega\, \omega\, \rho(\omega, k, -2) = 0.$$

$\rightsquigarrow$ 5-parameter ansatz:

$$\rho(\omega, k, -2) = \frac{A(1 + B\omega^2)\ \tanh(\omega\beta/2)}{[(\omega - \omega_0)^2 + b^2][(\omega + \omega_0)^2 + b^2][\omega^2 + a^2]}.$$

Analysis strategy: always determine B so as to satisfy the sum rule; scan over all other parameters to determine the χ^2 landscape.

For an early Backus-Gilbert analysis, see
Harris, Steinberg, Brandt, Francis, HM 1710.07050.

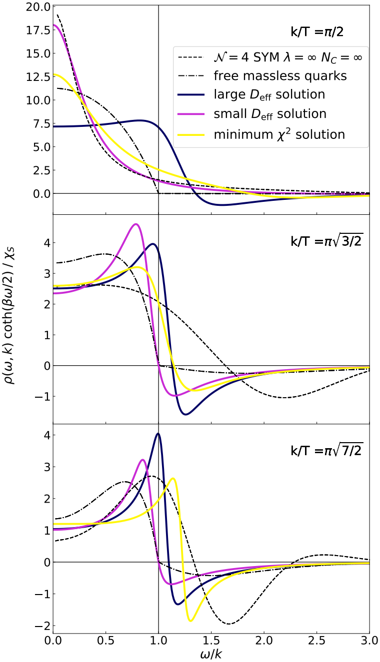

⟵ spec.funct. poorly constrained at small $k \simeq 0.4$ GeV

Representative spectral functions describing the lattice $2(T-L)$ correlator

⟵ spec.funct. better constrained at $k \approx 2\pi T \simeq 1.6$ GeV

Taking the continuum limit of $G_T(\tau, k)$

$\bar{G}_T(\tau, k) = G_T(\tau, k)/(T\chi_s)$

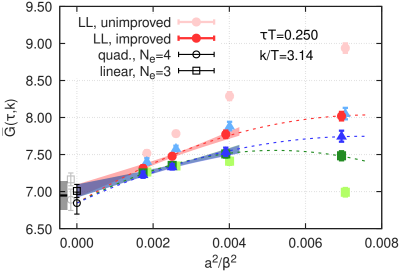

χ_s/T^2

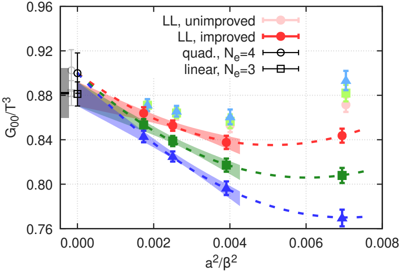

Three different discretisations, joint continuum extrapolation.

Use treelevel improvement.

Comparison of NLO+LPM spectral function to $T - L$ lattice data

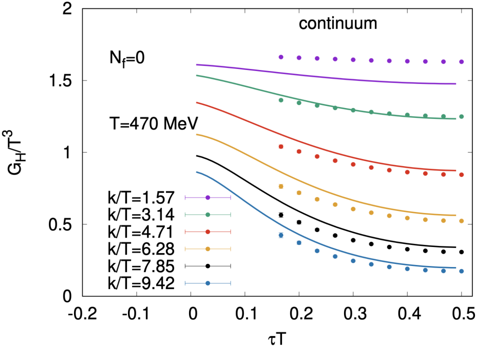

- Continuum-extrapolated quenched data from $N_t = 20, 24, 30$.
- General behaviour reproduced, but differences are visible.

2403.11647 Ali, Bala, Francis, Jackson, Kaczmarek, Turnwald, Ueding, Wink

Transverse-channel Euclidean correlator: lattice vs. NLO prediction

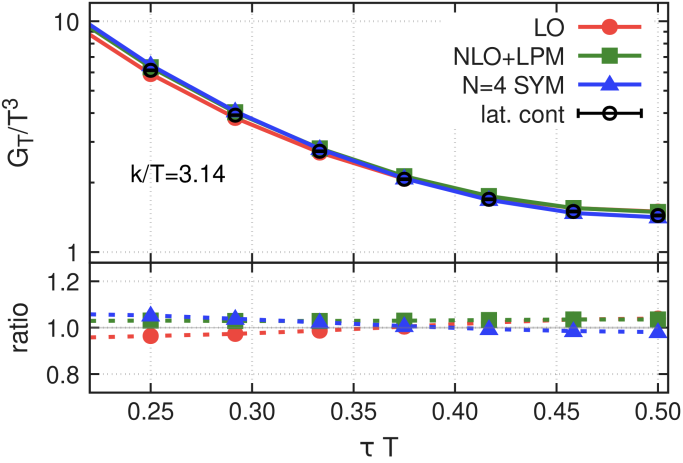

- NLO prediction lies a few percent higher than the lattice data.
- (For this comparison we set $\chi_s^{\rm AdS/CFT} = \frac{N_c^2 T^2}{8} \doteq \frac{9T^2}{8}$.)

NLO prediction based on Jackson, Laine 1910.07552.

Physically motivated fit ansätze for the spectral functions

$$\rho(\omega) = \rho_{\rm fit}(\omega)(1 - \Theta(\omega, \omega_0, \Delta)) + \rho_{\rm pert}(\omega)\Theta(\omega, \omega_0, \Delta)$$

with $\omega_0 \approx 2.5$ GeV the matching frequency (similar to Ghiglieri et al 1604.07544),

$$\Theta(\omega, \omega_0, \Delta) = (1 + \tanh[(\omega - \omega_0)/\Delta])/2$$

a smooth step function and $\rho_{\rm pert}(\omega)$ from [Jackson, Laine 1910.09567].

A) Polynomial ansatz:

$$\frac{\rho_{\rm fit,1}(\omega)}{T^2} = \sum_{n=0}^{N_{\rm p}-1} A_n \left(\frac{\omega}{\omega_0}\right)^{1+2n},$$

B) Piecewise polynomial ansatz:

$$\frac{\rho_{\rm fit,2}(\omega)}{T^2} = \begin{cases} A_0 \dfrac{\omega}{\omega_0} + A_1 \left(\dfrac{\omega}{\omega_0}\right)^3, & \text{if } \omega \le k, \\ B_0 \dfrac{\omega}{\omega_0} + B_1 \left(\dfrac{\omega}{\omega_0}\right)^3, & \text{if } \omega > k. \end{cases}$$

Representative lattice-QCD results for the spectral functions

Piecewise polynomial ansatz

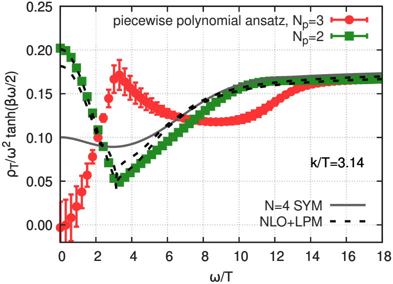

Polynomial ansatz

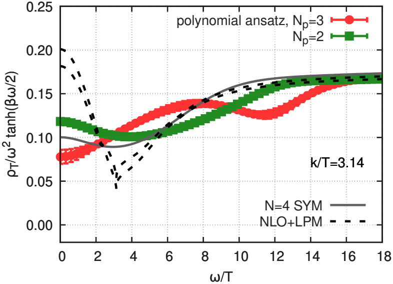

- Piecewise polynomial cannot 'decide' between having a min. or max. at $\omega = k$.
- Qualitatively, both the 'AdS/CFT' type and the 'NLO' type are compatible with the lattice data.